Chapter 8

Resonators with Internal Optical Elements

8.1 Resonators with Internal Lenses

We have seen in Sec. 5.1 that stable resonators exhibit large Gaussian beam radii if the resonator length is large or the g-parameters of the two mirrors are chosen close to a stability limit in the g-diagram. In both cases a large fundamental mode volume and, consequently, a high efficiency are obtained. In order to avoid a high misalignment sensitivity or a long resonator set-up, lenses can be used inside the resonator to enlarge the Gaussian beam radius in the active medium. Such a resonator with internal lenses is referred to as a lens resonator [3.182].

Let us first discuss the case in which only one lens with focal length f is located between the resonator mirrors as depicted in Fig. 8.1. If we calculate the ray transfer matrix for the transit from mirror 1 to mirror 2 we get (see Fig. 1.25 for the location of the reference planes):

$$M_D = \begin{pmatrix} g_1^* & L^* \\ \dfrac{g_1^* g_2^* - 1}{L^*} & g_2^* \end{pmatrix} \tag{8.1}$$

with:

$$g_i^* = g_i - D d_j (1 - d_j/\rho_i) \qquad i,j=1,2;\ i \neq j \tag{8.2}$$

$$L^* = d_1 + d_2 - D d_1 d_2 \tag{8.3}$$

$$D = 1/f \ : \ \text{refractive power}$$

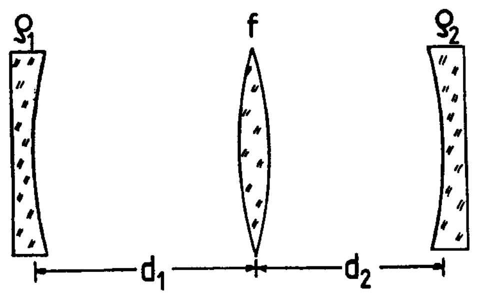

Fig. 8.1 Resonator with one internal lens.

Without the internal lens ($D=0$) the ray transfer matrix M_D becomes equivalent to the matrix M_0 of the empty resonator:

$$M_0 = \begin{pmatrix} g_1 & L \\ \dfrac{g_1 g_2 - 1}{L} & g_2 \end{pmatrix} \tag{8.4}$$

A comparison of the two ray transfer matrices indicates that a resonator with an internal lens exhibits the same ray transfer matrix for the transit as an equivalent, empty resonator with g-parameters g^*_1, g^*_2 and length L^*. Since the Gaussian beam radii at the mirrors are only a function of the ray transfer matrix elements, the lens resonator has the same Gaussian beam radii at the mirrors as the equivalent resonator. However, this equivalency holds only for the beam radii at the mirror planes. The beam caustic inside the lens resonator is different from that inside the equivalent resonator (the resonator in Fig. 8.1 exhibits two beam waists, one on each side of the lens). Since the Gaussian beam still exhibits a constant phase at the mirror surfaces the beam propagation inside the resonator can be easily calculated by using the Gaussian ABCD law (2.51).

Similar to empty resonators, lens resonators can be visualized in the equivalent g-diagram whose axes are defined by the g-parameters g^*_1 and g^*_2 (Fig. 8.2). Without an internal lens the resonator is located in the point (g_1,g_2). With increasing refractive power the location moves along a straight line through the g-diagram. The lens resonator is stable if the condition $0<g^*_1 g^*_2<1$ holds for the equivalent g-parameters. In the stable regions, the Gaussian beam radius at mirror i is given by:

$$w_i^2 = \frac{\lambda L^*}{\pi}\sqrt{\frac{g_j^*}{g_i^*(1-g_1^* g_2^*)}} \qquad i,j=1,2;\; i\neq j \tag{8.5}$$

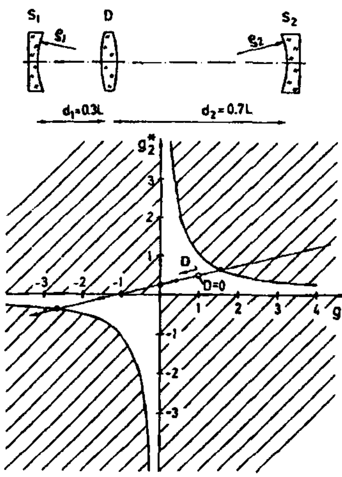

Fig. 8.2 Equivalent g-diagram of lens resonators. The resonator shown moves along the line as the refractive power is varied.

Example: semiconfocal resonator with $\rho_1=\infty$, ρ_2=2m, L=1m, λ=500nm

a) Without an internal lens we obtain:

g_1=1.0 and g_2=0.5

According to (8.5), the Gaussian beam radii at the mirrors are given by:

w_1=0.399mm and w_2=0.798mm

b) Insertion of a negative lens with focal length f=-2m at the position d_1=0.8m results in the equivalent resonator parameters:

g^*_1=1.1, g^*_2=0.86, L^*=1.08m

The lens resonator is stable since the product of the equivalent g-parameters is 0.946. Equation (8.5) yields for the Gaussian beam radii at the mirrors:

w_1=0.809mm and w_2=0.915mm

If more than one lens is located inside the resonator the beam radii at the mirrors can be determined in a similar way. After calculating the ray transfer matrix for a resonator transit starting at mirror 1 (the reference plane is the mirror surface):

$$M = \begin{pmatrix} A & B \\ C & D \end{pmatrix}$$

the equivalent g-parameters and the equivalent resonator length can be defined as:

$$g_1^* = A\ , \qquad g_2^* = D\ , \qquad L^* = B$$

and the Gaussian beam radii are again given by (8.5). A commonly used lens resonator with two lenses is the telescope resonator [3.194] (Fig. 8.3). This resonator comprises a telescope of magnification $M=|f_2/f_1|$ and length $\ell=f_1+f_2$, which increases the beam radius at mirror 2 and decreases the beam radius at mirror 1. The equivalent resonator parameters read:

$$g_1^* = M - \frac{L^*}{\rho_1}\ , \qquad g_2^* = \frac{1}{M} - \frac{L^*}{\rho_2}\ , \qquad L^* = \ell + d_1 M + \frac{d_2}{M}$$

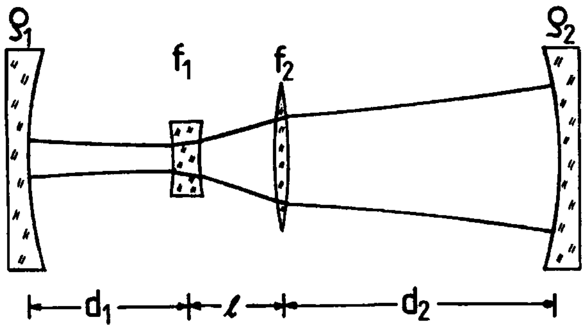

Fig. 8.3 Telescope resonator.

8.2 Resonators with Polarizing Elements

A resonator which consists only of mirrors is degenerated as far as the polarization of the emitted beam is concerned. All oscillation directions of the electromagnetic radiation exhibit the same probability and the resonator will therefore emit unpolarized light. This means that the polarization vector varies statistically with a time constant determined by perturbations of the resonator set-up and the physical properties of the active medium. By inserting polarizing elements into the resonator a well-defined polarization can be generated resulting in a polarized electric field which is reproduced after each round trip. Examples of polarizing intracavity elements are birefringent lenses, retardation plates, and polarizers. In most lasers, the active medium itself will also affect the polarization, either due to inherent or pump induced birefringence, or due to the special geometry of the end faces.

The theoretical treatment of the polarization was already discussed in Chapter 3. The influence of an optical element on the polarization can be mathematically described by using 2x2 matrices which relate the input and the output polarization vector to each other [3.181]. In the following we summarize the main results of the Jones matrix formalism. In optical resonators, the polarization is determined by the resulting Jones matrix M^P for a round trip. The polarization is characterized by the field vector $\boldsymbol{E}$ whose components represent the field amplitudes in the two perpendicular directions. If a cartesian coordinate system is used, the field vector is defined by the amplitudes in the x- and the y-direction and the relative phase shift Φ in between:

$$\boldsymbol{E} = \begin{pmatrix} E_{0x} \\ E_{0y}\ \exp[i\phi] \end{pmatrix} \tag{8.6}$$

For circularly symmetric optical elements it is convenient to express the field vector in radial and azimuthal components:

$$\boldsymbol{E}_r = \begin{pmatrix} E_{0r} \\ E_{0\phi}\ \exp[i\phi] \end{pmatrix} \tag{8.7}$$

In both coordinate systems the two field vectors $\boldsymbol{E}_1,\boldsymbol{E}_2$, which are eigenvectors of the Jones matrix, represent the eigenstates of the polarization with:

$$\mu_i^P \boldsymbol{E}_i = \boldsymbol{M}^P \boldsymbol{E}_i \tag{8.8}$$

The eigenvalue μ_i determines the loss factor per round trip V for the corresponding field vector $\boldsymbol{E}_i$:

$$V = \mu_i \mu_i^* \tag{8.9}$$

In general only the polarization exhibiting the lower loss factor will be observed. If the Jones matrix M^P in the x-y coordinate system is known, the Jones matrix M_r^P in the polar coordinate system is given by:

$$M_r^P = \begin{pmatrix} \cos\theta & \sin\theta \\ -\sin\theta & \cos\theta \end{pmatrix} M^P \begin{pmatrix} \cos\theta & -\sin\theta \\ \sin\theta & \cos\theta \end{pmatrix} \tag{8.10}$$

with $x=r\cos\theta$ and $y=r\sin\theta$. The corresponding transformation rule for the field vectors (8.6) and (8.7) reads:

$$E_r = \begin{pmatrix} \cos\theta & \sin\theta \\ -\sin\theta & \cos\theta \end{pmatrix} E \tag{8.11}$$

The eigenvalue equation (8.8) holds in both coordinate systems if the Jones matrix and the field vector are transformed according to (8.10) and (8.11), respectively. If the resulting Jones matrix M^P for the resonator round trip is given in the general form:

$$M^P = \begin{pmatrix} m_{11} & m_{12} \\ m_{21} & m_{22} \end{pmatrix}$$

the eigenvalues and the eigenvectors can be calculated by using the relations:

$$\mu_{1,2}^P = \frac{m_{11}+m_{22}}{2} \pm \sqrt{\left(\frac{m_{11}-m_{22}}{2}\right)^2 + m_{12}m_{21}} \tag{8.12}$$

$$E_i^P = \begin{pmatrix} 1 \\ \dfrac{\mu_i^P - m_{11}}{m_{12}} \end{pmatrix} ; \qquad i=1,2 \qquad \textit{if} \;\; m_{12} \neq 0 \tag{8.13}$$

$$E_1^P = \begin{pmatrix} 1 \\ 0 \end{pmatrix}, \; E_2^P = \begin{pmatrix} 1 \\ 0 \end{pmatrix}; \quad i=1,2 \qquad \textit{if} \;\; m_{12} = m_{21} = 0 \tag{8.14}$$

The resulting Jones matrix for the resonator round trip is obtained by multiplying the Jones matrices of all elements in the same sequence as the elements are passed. Thus, the Jones matrix of the first element stands on the right hand side of the matrix product. For a collection of Jones matrices see Chapter 3. In the following sections, common optical resonators with polarizing elements are discussed using the Jones matrix formalism.

8.2.1 The Twisted Mode Resonator

This resonator employs a polarizer and two quarter wave plates whose fast axes are rotated by +45° and -45° with respect to the transmission direction of the polarizer (we chose the y-axis). The resulting Jones matrix for the round trip starting at the left mirror reads:

$$M^P = M_P^P\, M_R^P(45°)\, M_R^P(-45°)\, M_R^P(-45°)\, M_R^P(45°)\, M_P^P = \begin{pmatrix} 0 & 0 \\ 1 & 0 \end{pmatrix}$$

In the y-direction linearly polarized light exhibits no losses in the resonator and the field vector is reproduced after each round trip. Starting at mirror 1 the field becomes right-circularly polarized by the first λ/4 plate, and after passage through the second λ/4 plate the beam is again linearly polarized in the y-direction at the output coupling mirror. On the way back to the HR mirror the beam is transformed into a left-circularly polarized beam between the retardation plates. Due to the different circularity inside the medium of the back and the forth travelling wave, no interference between these waves can occur. The generation of standing waves is thus prevented and the time-averaged intensity is constant along the length of the active medium [3.191]. This lack of spatial hole burning stabilizes the temporal laser emission since the interaction between axial modes is missing. In homogeneously broadened lasers, this resonator provides single axial mode operation. The twisted mode resonator can also be used in frequency doubled Nd:YAG lasers to prevent chaotic laser emission at 532nm due to axial mode competition, often referred to as the "green problem".

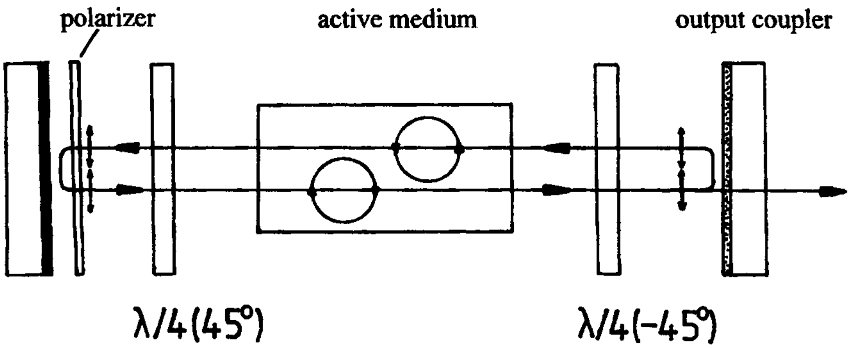

Fig. 8.4 The twisted mode resonator. Two quarter wave plates generate right-circular and left-circular polarization for the forth and the back travelling waves, respectively. At both mirrors the field is linearly polarized in the y-direction.

8.2.2 Resonators with Variable Output Coupling

If only one quarter wave plate is used in the twisted mode resonator of Fig. 8.4, the linearly polarized field vector is rotated by 90° after the round trip. The loss factor is then equal to zero and all the intracavity power is coupled out of the resonator. By rotating the quarter wave plate the loss factor can be continuously varied between 0 and 1 resulting in a variable output coupling (Fig. 8.5). If the rotation angle α is defined by the angle between the fast axis of the quarter wave plate and the transmission direction of the polarizer, no output coupling (loss factor of 1.0) is attained at angles α of 0°, 90°, 180°, and 270°, whereas maximum output coupling is observed at 45°, 135°, 225°, and 315°. Rotation of the $\lambda/4$ plate thus enables one to vary the output power of the laser.

Let us consider the general case that the retardation plate induces an arbitrary phase shift δ between the principal axes (Fig. 8.5). Starting at the left mirror, the resulting Jones matrix reads (transmission direction of the polarizer is the y-direction):

$$M^P = M_P^P \, M_R^P(\alpha) \, M_R^P(\alpha) \, M_P^P$$

$$= \begin{pmatrix} 0 & 0 \\ 1 & [\cos\alpha\sin\alpha(1-\exp[i\delta])]^2 + [\sin^2\alpha + \exp[i\delta]\cos^2\alpha]^2 \end{pmatrix} \tag{8.15}$$

The loss factor per round trip is given by:

$$V = 1 - [\sin\delta\sin2\alpha]^2 := 1 - R \tag{8.16}$$

with R being the reflectance of the polarizer which corresponds to the reflectance of the output coupling mirror in a standard resonator.

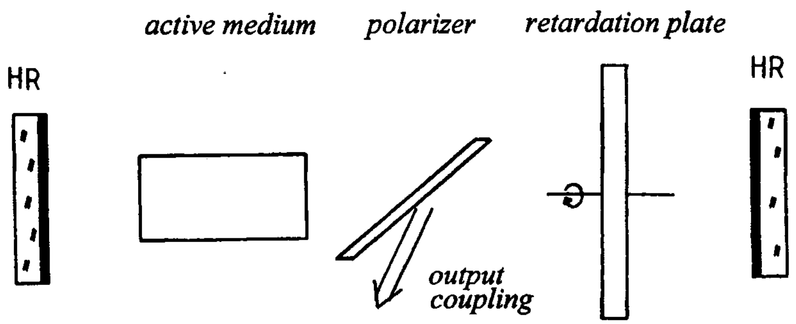

Fig. 8.5 Resonator with internal polarizer and rotatable retardation plate. The polarizer reflects the field component oscillating perpendicular to its transmission direction out of the resonator. The angle of rotation of the retardation plate determines the output coupling.

The upper graph of Fig. 8.6 presents the measured and the calculated loss factor per round trip for a retardation plate with δ=73° as a function of the angle of rotation α. Measured output energies per pulse of a Nd:YAG laser utilizing this retardation plate are shown in the lower diagram. There are two advantages of this resonator concept. First, the output power can be varied without changing the pump power. Variations in mode structure and focusability caused by the change in pump power can thus be avoided. Secondly, the output coupling of the resonator can be adjusted so that the maximum output power is obtained for any value of the pump power. In Fig. 8.6, the rotation angle has to be changed from 12° to 22° as the pump energy is increased to always attain maximum output energy. This is in contrast to resonator schemes with an output coupling mirror which provide optimum output coupling only at one value of the pump power (see Chapter 10).

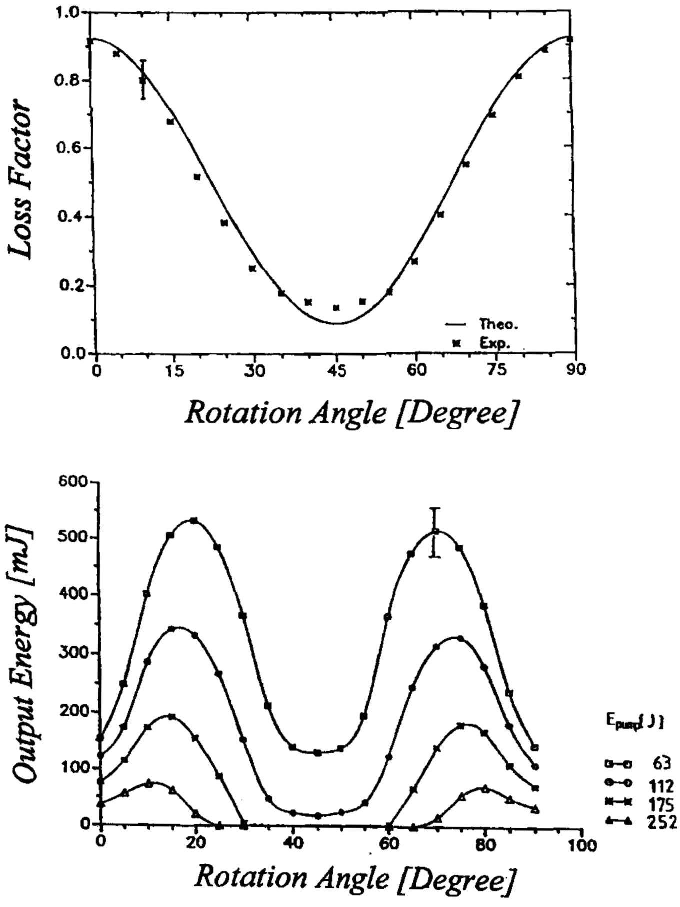

Fig. 8.6 Measured and calculated dependence of the loss factor and the output energy of a pulsed Nd:YAG rod laser (repetition rate: 0.5Hz) as a function of the angle of rotation α of the retardation plate (δ=73°). The curve parameter in the lower diagram is the pump energy [S.10].

8.2.3 Pockels Cell Resonator

Instead of rotating a retardation plate to change the output coupling it is also possible to use a Pockels cell with varying voltage U [3.190] (Fig. 8.7). A Pockels cell consists of a nonlinear crystal to which a voltage in the kV range is applied. A Pockels cell acts as a retardation plate whose principal axes are rotated by 45° with respect to the direction of the applied electric field. The phase shift δ is a linear function of the voltage U:

$$\delta = \frac{U}{U_{\lambda/4}} \frac{\pi}{2} \tag{8.17}$$

The quarter wave voltage $U_{\lambda/4}$ is a characteristic of the Pockels cell and it denotes the voltage required to generate the characteristics of a $\lambda/4$ plate (typically in the multi kV range). The resulting Jones matrix for the resonator round trip, starting at the polarizer, is given by:

$$\begin{aligned} M^P &= M_P^P\, M_R^P(45^\circ)\, M_R^P(45^\circ)\, M_P^P \\ &= \begin{pmatrix} 0 & 0 \\ 0 & \cos\delta \end{pmatrix} \end{aligned} \tag{8.18}$$

Therefore, the loss factor per round trip is given by V=$\cos^2\delta$ which results in a reflectance R of the polarizer of:

$$R = 1 - V = \sin^2\left[\frac{\pi U}{2U_{\lambda/4}}\right] \tag{8.19}$$

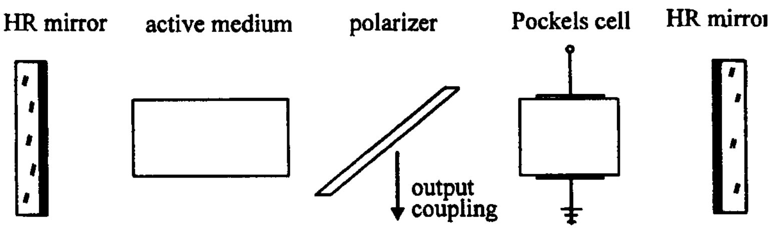

Fig. 8.7 Pockels cell resonator. The Pockels cell acts like a retardation plate whose principal axes are rotated by 45°. The phase shift δ can be varied with the applied voltage.

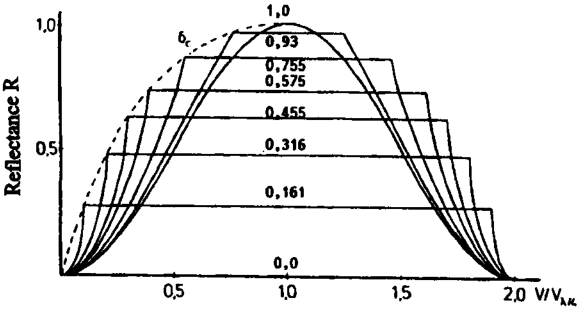

Fig. 8.8 Reflectance R of the polarizer as a function of the Pockels cell voltage. The curve parameter is the degree of polarization P of the polarizer.

The sinusoidal variation of the reflectance R can only be observed for polarizers with an ideal degree of polarization of P=1.0 (see Sec. 1.3). As the degree of polarization is decreased, regions of constant reflectance develop as shown in Fig. 8.8.

The Pockels cell resonator has found widespread application in lasers generating short pulses in the ns-range. The beam is coupled out of the resonator via a standard output coupling mirror and the polarizer is only used to generate a high loss. This loss can be suddenly decreased by switching off the Pockels cell. (Fig. 8.9). If the quarter wave voltage is applied, the linear polarization is rotated by 90° after a round trip resulting in a reflectance of 100% at the polarizer. In this configuration the laser threshold cannot be reached and the pump process keeps building up the inversion inside the active medium. As soon as the steady state inversion is reached the voltage at the Pockels cell is switched off (switching times are on the order of ns) and the reflectance of the polarizer is decreased to a value close to zero. The laser will start oscillating and the high inversion is depleted by a short, intense light pulse with a duration in the 10-100 ns range. Since the cavity Q of the resonator is changed from a very low to a high value, this technique is referred to as Q-switching. In cw pumped lasers the switching frequencies using Pockels cells can be as high as 50kHz. If a pulsed pump source is used, the switching of the Pockels cell is usually in synchronization with the pump frequency (in the range of 1-1000 Hz). In high power lasers, the absorption losses of a Pockels cell are too high resulting in beam distortion and even damage. Therefore, in most commercial lasers acousto-optical elements are used which generate losses due to diffraction by an acoustically excited refractive grating.

Another way to rapidly change the resonator loss is the use of a saturable absorber whose transmission is a function of the light intensity (passive Q-switching). The nonlinear transmission is caused by dye molecules which are either dissolved in a fluid or embedded in a transparent foil or by a doped solid state material (e.g. Cr:YAG). This technique is easier to realize since no switching of high voltages is required. Passive Q-switching is, therefore, used in some commercial systems. However, the Q-switching cannot be actively controlled and the repetition rate is determined by the net round trip gain of the resonator. In addition, absorption in the Q-switch material limits this method to low power lasers (<10W).

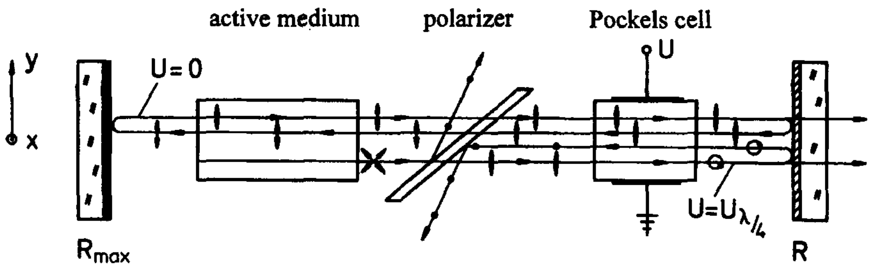

Fig. 8.9 Pockels cell resonator for the generation of short pulses via Q-switching. If the quarter wave voltage is applied to the Pockels cell, the laser cannot oscillate due to the high reflectance of the polarizer. After the voltage is switched off the inversion in the active medium is depleted by a short, intense light pulse.

8.2.4 Resonators with Radially Birefringent Elements

A radially birefringent element is a retardation plate whose phase shift δ is a function of the radial distance r from the optical center. The radial dependence is generated by changing the thickness of the retardation plate with increasing radius. Preferably one surface of the plate is curved with a radius of curvature ρ generating a birefringent lens (Fig. 8.10). If n_1 and n_2 denote the indices of refraction along the two principal axes ($n_2>n_1$), an electric field polarized linearly along the axis i experiences the phase shift:

$$\delta_i(r) = \frac{2\pi}{\lambda} n_i \left(d_0 + \frac{r^2}{2\rho} \right) \tag{8.20}$$

Note that the refractive power of the lens depends on the polarization. However, the difference between the two indices of refraction is usually very small (less than one %) and the polarization effect on the refractive power can therefore be neglected. If the slow axis coincides with the y-axis of the reference frame, the Jones matrix of the radially birefringent lens reads:

$$M_{RB} = \begin{pmatrix} 1 & 0 \\ 0 & \exp[i\delta(r)] \end{pmatrix} \tag{8.21}$$

with: $$\delta(r) = \frac{2\pi}{\lambda}(n_2 - n_1)\left[d_0 + \frac{r^2}{2\rho} \right]$$

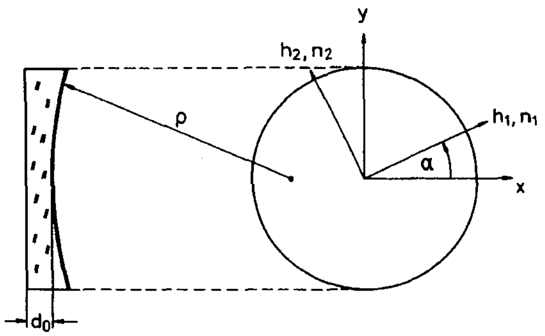

Fig. 8.10 Radially birefringent element. Electric fields that are linearly polarized along the two principal axes h_1 and h_2 experience different indices of refraction n_1 and n_2. The thickness of the element is a function of the radial coordinate.

The Jones matrix is the same as the one for a retardation plate except for the radial dependence of the phase shift. If we replace the retardation plate in the resonator with variable output coupling (Fig. 8.5) by the birefringent lens (Fig. 8.11), the loss factor becomes a function of the radius r:

$$V(r) = 1 - [\sin(\delta(r))\sin 2\alpha]^2 \tag{8.22}$$

Thus, the birefringent lens generates a radially variable output coupling [3.193]. The combination lens-polarizer-mirror simulates a variable reflectivity mirror (VRM) with reflectivity profile $R=V(r)$. This resonator set-up was used for the first demonstration of an unstable resonator with VRM [3.193,3.195]. The angle of rotation α of the lens and its center thickness d_0 can be used to vary the shape of the reflectivity profile. Figure 8.12 shows calculated loss factor profiles $V(r)$ for a quartz lens with a radius of curvature of 1m. The thickness d_0 was chosen such that the loss factor $V(0)$ at the center is equal to 1.0 ($d_0\Delta n/\lambda$ is an integer value). By changing d_0 arbitrary values for the center loss factor can be generated.

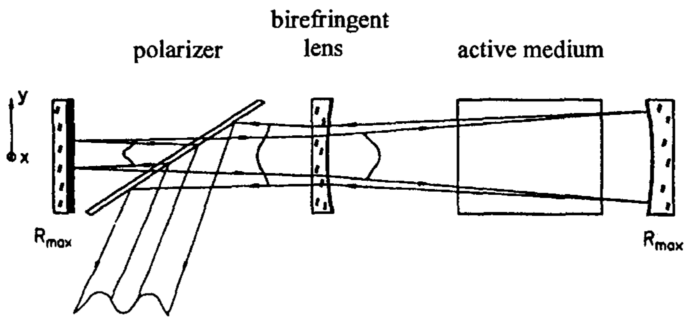

Fig. 8.11 Resonator with radially birefringent lens. The radial dependence of the phase shift generates a radially variable output coupling.

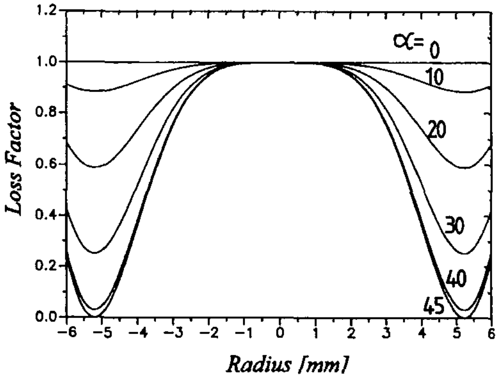

Fig. 8.12 Radial loss factor profiles (8.22) of the resonator shown in the previous figure for a quartz lens (n_2-n_1=0.0092, ρ=1m) and a wavelength of λ=500nm. The curve parameter is the angle of rotation α. The system simulates a VRM with reflectance profile $V(r)$.

8.2.5 Resonators with Azimuthally Birefringent Elements

Azimuthally birefringent materials exhibit different indices of refraction n_r and n_θ for radially and azimuthally polarized light (Fig. 8.13). If in the y-direction linearly polarized light is incident on such an optical element, the field vector has different components in the radial and the azimuthal direction and the relative amplitudes of the two components depend on the azimuthal angle θ. After passage through the birefringent material, the polarization state is a function of the angle θ. Azimuthal birefringence is observed in pumped solid state laser rods [3.2,3.186,3.188].

If $\delta=2\pi\ell(n_r-n_\theta)/\lambda$ denotes the relative phase shift between the r- and the θ-component of the field vector, the Jones matrix for the azimuthally birefringent material reads in polar coordinates:

$$M_{ABr}^{P} = \begin{pmatrix} \exp[i\delta] & 0 \\ 0 & 1 \end{pmatrix} \tag{8.23}$$

By applying the transformation (8.10), the Jones matrix in the cartesian reference frame is obtained:

$$M_{AB}^{P} = \begin{pmatrix} \cos\theta & -\sin\theta \\ \sin\theta & \cos\theta \end{pmatrix} M_{Abr}^{P} \begin{pmatrix} \cos\theta & \sin\theta \\ -\sin\theta & \cos\theta \end{pmatrix}$$

$$= \begin{pmatrix} \exp[i\delta]\cos^2\theta + \sin^2\theta & (\exp[i\delta]-1)\sin\theta\cos\theta \\ (\exp[i\delta]-1)\sin\theta\cos\theta & \exp[i\delta]\sin^2\theta + \cos^2\theta \end{pmatrix} \tag{8.24}$$

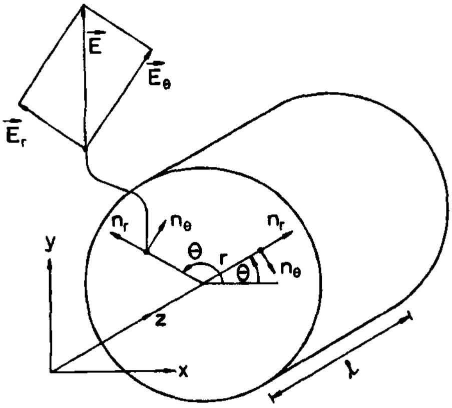

Fig. 8.13 Azimuthally birefringent element. Radially and azimuthally polarized fields experience different indices of refraction n_r and n_θ. After passage through the element, linearly polarized light exhibits a polarization state which depends on the azimuth θ.

The elements of the Jones matrix depend only on the azimuthal angle θ. If the active medium exhibits azimuthal birefringence, output coupling via a polarizer will therefore generate a beam profile with an azimuthal structure. By using the resulting Jones matrix for the resonator round trip, the loss factor can be calculated to be:

$$V(\theta) = 1 - [\sin\delta\sin2\theta]^2 = 1 - R(\theta) \tag{8.25}$$

The output coupling is maximum (minimum loss factor V and maximum reflectance R) at the angles θ of 45°, 135°, 225°, and 315°. The beam profile thus looks like a Maltese cross rotated by 45°. Note that a rotation of the azimuthally birefringent element does not change the output pattern. The average reflectance R of the polarizer is obtained by integrating the reflectance $R(\theta)$ over the azimuthal angle:

$$R = \frac{1}{2\pi}\int_0^{2\pi} R(\theta) d\theta = \frac{1}{2}\sin^2\delta \tag{8.26}$$

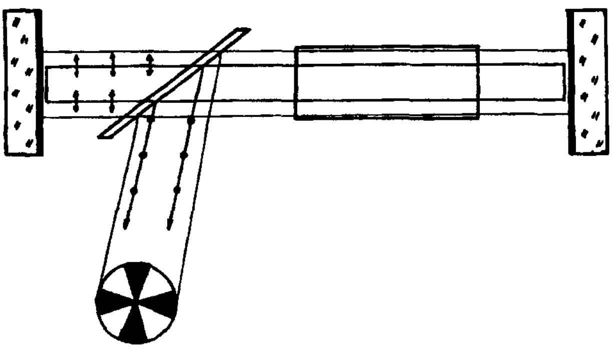

Fig. 8.14 Resonator with polarizer and azimuthally birefringent element. The output coupling depends on the azimuthal angle θ.

8.2.6 Resonators with Radial-Azimuthally Birefringent Elements

In many solid state laser rods, radial and azimuthal birefringence are generated simultaneously by the pump process. The azimuthal intensity pattern coupled out by the polarizer thus exhibits radial rings whose number increase with increasing pump power (Fig. 8.15). The combination of heat generation due to absorption of pump radiation and the flow of heat to the outer periphery due to cooling leads to a parabolic radial temperature profile. The induced stress generates azimuthal birefringence and the temperature profile leads to a radial decrease of both indices of refraction:

$$n_r(r) = n_0\,(1 - \gamma_r r^2)\,, \qquad n_\theta(r) = n_0\,(1 - \gamma_\theta r^2) \tag{8.27, 8.28}$$

The shape factors γ_r and γ_θ are proportional to the average pump power. The pumped laser rod acts like a lens with refractive powers D_r and D_θ for the two polarizations. If end effects are neglected, the refractive powers for a rod of length ℓ read in a first order approximation:

$$D_r = 2\gamma_r n_0 \ell\,, \qquad D_\theta = 2\gamma_\theta n_0 \ell \tag{8.29, 8.30}$$

The Jones matrix of the laser rod can now be determined by inserting (8.27)-(8.30) into the Jones matrix (8.24) of the azimuthally birefringent element:

$$M_{LR}^{P} = \begin{pmatrix} \exp[i\delta(r)]\cos^2\theta + \sin^2\theta & (\exp[i\delta(r)]-1)\sin\theta\cos\theta \\ (\exp[i\delta(r)]-1)\sin\theta\cos\theta & \exp[i\delta(r)]\sin^2\theta + \cos^2\theta \end{pmatrix} \tag{8.31}$$

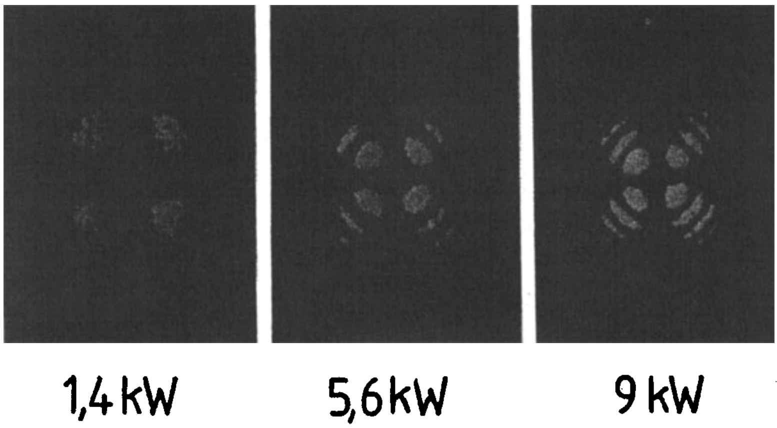

Fig. 8.15 Photographed intensity distributions generated by a collimated HeNe laser beam after passage through a pumped Nd:YAG rod. The rod is placed between crossed polarizers. The parameter is the electrical pump power [S.10].

with $$\delta(r) = -\frac{\pi}{\lambda}(D_r - D_\theta)r^2 = -\frac{\pi}{\lambda}\Delta D r^2 \tag{8.32}$$

For a flashlamp pumped Nd:YAG rod with radius b=5mm typical values for the refractive powers per kW of electrical pump power are D_r=0.3 m^{-1} and D_θ=0.255m^{-1}.
By introducing the thermal lensing coefficient α [3.195] (see Sec. 12.1):

$$\alpha = \frac{(D_r + D_\theta)}{2}\frac{\pi b^2}{P_{pump}} = \frac{D_{ave}\pi b^2}{P_{pump}} \tag{8.33}$$

where we introduced the average refractive power D_{ave}. and the pump power P_{pump} The phase shift (8.32) can be rewritten as:

$$\delta(\eta) = -\frac{\beta}{\lambda}\alpha P_{pump}\,\eta^2 \tag{8.34}$$

where we used the relation $\Delta D = \beta D_{ave}$ ($\beta<1$, $\beta\approx0.15$ for Nd:YAG) and η=r/b is the normalized radial coordinate. Equation (8.34) indicates that for the same pump power, the radial phase shift in the rod is the same, independent of the rod radius. For Nd:YAG, typical values of the thermal lensing coefficient are 0.1-0.15 µm/W for diode pumping (P_{pump}: optical pump power) and 0.02-0.03 µm/W for flashlamp pumping (P_{pump}: electrical pump power), depending on doping concentration and pump light spectrum.

If a polarizer is placed inside the resonator to generate a linearly polarized beam (as in Fig. 8.14), the loss factor per round trip is a function of r and θ. According to (8.25) the reflectance of the polarizer reads:

$$R(\eta,\theta) = [\sin\delta(\eta)\sin2\theta]^2 \tag{8.35}$$

The total loss R per round trip due to reflection at the polarizer can be calculated by integrating (8.32) over the radial and the azimuthal coordinates:

$$R = \frac{1}{\pi}\int_0^{2\pi}\int_0^1 [\sin\delta(\eta)\sin2\theta]^2\eta\,d\eta\,d\theta = \frac{1}{4}\left[1 - \frac{\sin x}{x}\right] \tag{8.36}$$

with $x=2\delta(\eta=1)$. Figure 8.16 shows the graphic presentation of (8.36). Amazingly, for high pump powers the loss per round trip converges towards a value of 25% which means that only a quarter of the intracavity power is coupled out. An experimental verification of this effect is presented in Fig. 8.17. A Nd:glass rod was placed between crossed polarizers and the transmitted power P of a collimated Nd:glass laser beam was measured as a function of the electrical pump power. The solid line represents the theoretical dependence given by (8.36) with $x=\delta(\eta=1)$ (the factor 2 is missing because only the loss for a transit is measured). Note that a smaller rod radius b does not reduce the loss since $b^2 \Delta D$ is a constant of the laser head. However, it is possible to decrease the loss by inserting an aperture (radius a) to reduce the beam size. In this case, (8.34) has to be multiplied by a^2/b^2.

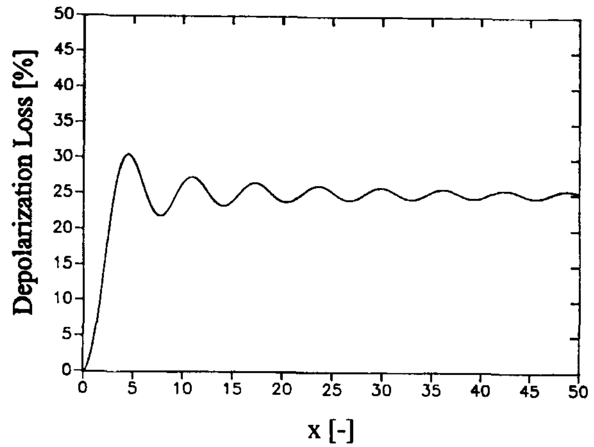

Fig. 8.16 Calculated loss per round trip of resonators with a radial-azimuthally birefringent medium and an intracavity polarizer, according to (8.36). The loss is generated by output coupling at the polarizer.

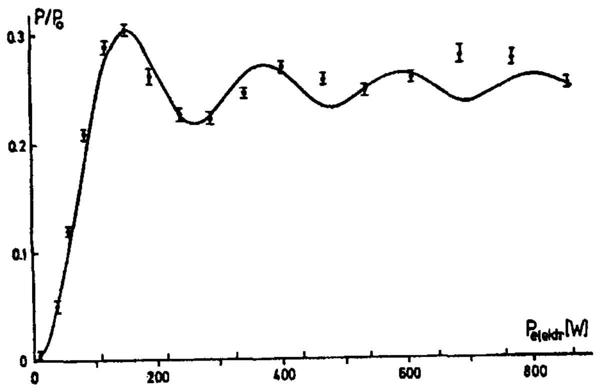

Fig. 8.17 Measured and calculated dependence of the transmitted power P of a Nd:glass laser beam passing through a pumped Nd:glass rod as a function of the electrical pump power. The Nd:glass rod is placed between crossed polarizers. The power P is normalized with respect to the power P_0 obtained for parallel polarizers and no pumping [S.10].

8.2.7 Compensation of Radial-Azimuthal Birefringence

The treatment of radial-azimuthal birefringence is important to estimate the influence of the birefringence on the performance of solid state laser resonators. There are two main effects of birefringence on the laser properties. First, generation of a linearly polarized output by placing a polarizer into the resonator will result in losses and, consequently, a considerable decrease in output power. Secondly, the different refractive powers for radially and azimuthally polarized fields result in different beam propagation for the two fields inside the resonator. This leads to a deterioration of the beam quality [3.198] and a decrease of the mode volume inside the active medium.

It is therefore very important to come up with resonator schemes that provide an intracavity compensation of the thermally induced birefringence [3.185,3.196-199,3.205,3.209]. The basic idea of birefringence compensation is the rotation of the field vector by 90° between transits through the active medium. The rotation switches the r- and the θ-component of the field and the second transit will then equalize the phase shifts experienced by the two components. This means that both polarizations experience the same refractive power of $D_{ave}=(D_r+D_\theta)/2$.

If two rods are used, the rotation can be accomplished by placing a 90° quartz rotator between the rods (Fig. 8.18a). This technique of birefringence compensation was patented in 1969 [3.185] and first demonstrated in 1971 in a dual rod flashlamp pumped TEM_{00} mode Nd:YAG laser [3.187]. Alternatively, the quartz rotator can be replaced by two half wave plates whose principal axes are rotated by 45° with respect to one another (see Sec. 3.2.3).This may be a good alternative if the space between the rods is limited, since a quartz rotator has a length of appr. 14mm at 1064nm.

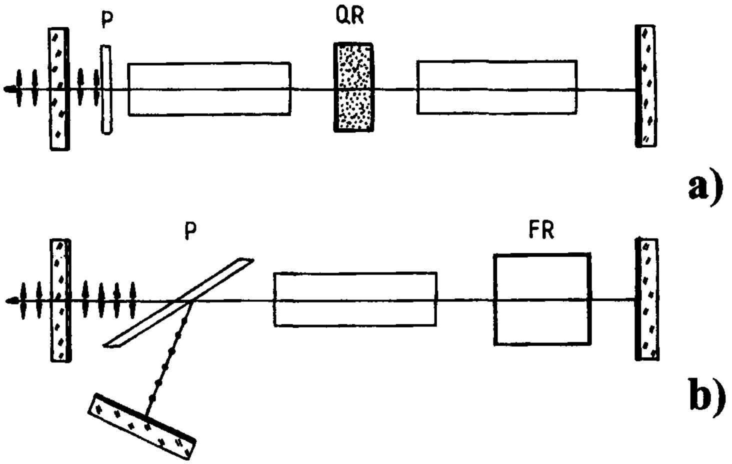

Fig. 8.18 Resonators with birefringence compensation for the generation of linearly polarized output. a) dual rod resonator with 90° quartz rotator (QR), b) single rod resonator with 45° Faraday rotator (FR).

For resonators with a single rod, a 45° Faraday rotator located between the rod and the HR mirror has to be used (Fig. 8.18b). Note that a 45° quartz rotator will not work in this case because the rotation is canceled when the wave passes the rotator the second time on its way back to the rod. After one round trip in the resonator the light is again linearly polarized but with an oscillation direction which is rotated by 90°. The polarizer now totally reflects the beam and an additional mirror feeds the beam back into the resonator. Another round trip will then generate the initial linear polarization state again. This compensation scheme thus requires four transits through the active material. By adding a second 45° Faraday rotator between the laser rod and the polarizer, the reflection at the polarizer can be prevented [3.209].

Unfortunately, Faraday rotators are relatively expensive devices. More affordable is the poor man's version of a Faraday rotator compensation scheme as depicted in Fig. 8.19 [3.214]. The p- and the s- polarized components of the beam are separated by a polarization cube and recombined after rotating each linear polarization component by 90°. To the authors' best knowledge, there has not been an experimental verification of this set-up yet.

A simple technique to partially compensate the birefringence at lower pump powers is depicted in Fig. 8.20 [3.203,3.205,3.207]. The quarter wave plate has its principal axes aligned parallel and perpendicular to the transmission direction of the polarizer. Fig. 8.21 shows calculated loss per roundtrip at the polarizer as a function of pump power for a diode pumped Nd:YAG rod (α=0.15μm/W, β=0.15 in (8.35)) both for a flat-top beam profile and a Gaussian TEM_{00} mode. This compensation technique is useful for low gain, low power lasers with diode pump powers and flashlamp pump powers of up to 100W and 1kW, respectively, where any loss in the cavity has a considerable effect on the output power. Examples are the 946nm, 1319nm and 1444nm transitions in Nd:YAG.

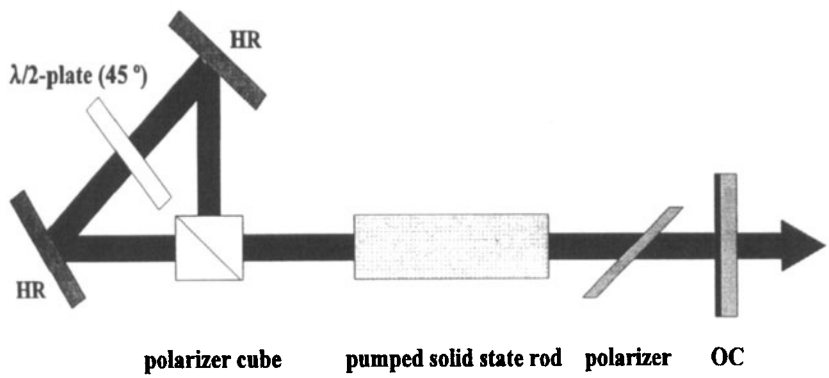

Fig. 8.19 Poor man's Faraday rotator using a half wave plate with its principal axes rotated by 45°.

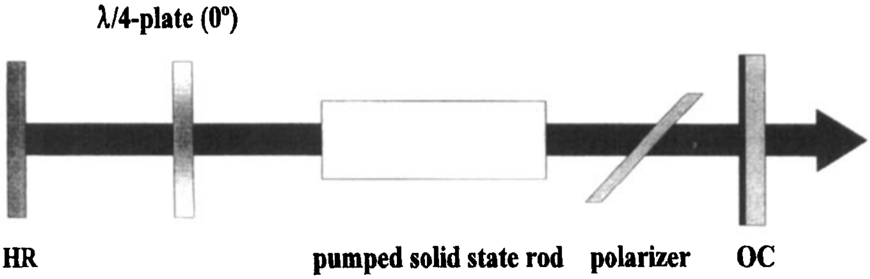

Fig. 8.20 Partial birefringence compensation in a single rod resonator using a quarter wave plate.

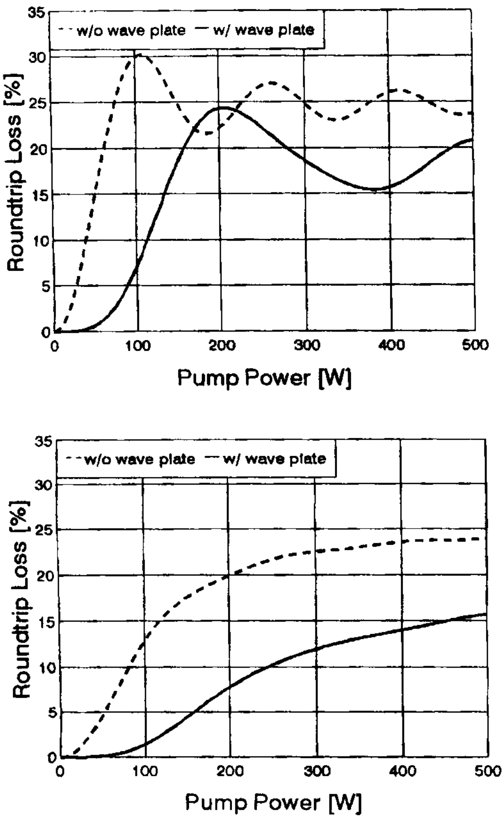

Fig. 8.21 Calculated roundtrip loss for the resonator of Fig. 8.20 with and without the quarter wave plate inserted as a function of the absorbed diode pump power (Nd:YAG, α=0.15μm/W, β=0.15). Top: Flat top beam filling the entire crod cross-section, bottom: Gaussian TEM_{00} mode with beam radius of 0.7 times the rod radius.

Unfortunately, the resonator schemes presented in Figs. 8.18 and 8.19 will not completely compensate for birefringence as the pump power is increased. Due to thermal focusing, the rays propagate through the active medium not parallel to its axis and differently in both rods, or for a single rod resonator, the rays intersect the rod differently during the second transit. Since the phase shift is a function of the radial and the azimuthal coordinate it is necessary that a ray passes through the rod at the same coordinates after the oscillation direction is rotated. By using transformation optics between the rods it is theoretically possible to achieve perfect birefringence compensation by matching the beam propagation in the two rods [3.199] (Fig. 8.22). These compensation schemes can also be applied to single rod resonators, but the imaging property of the rear resonator mirror has to be incorporated.

a) Single Lens Scheme (Fig. 8.22a)

With one focusing lens of focal length f located at distances d_1 and d_2 from the end faces of the rods, perfect birefringence compensation will occur if the following conditions hold [3.199]:

$$d_1 = d_2 = f - \frac{\ell}{2n_0} + \sqrt{f^2 - \left[\frac{\ell}{2n_0}\right]^2} \tag{8.37}$$

where ℓ is the length of the rod and n_0 is the index of refraction at the rod center.

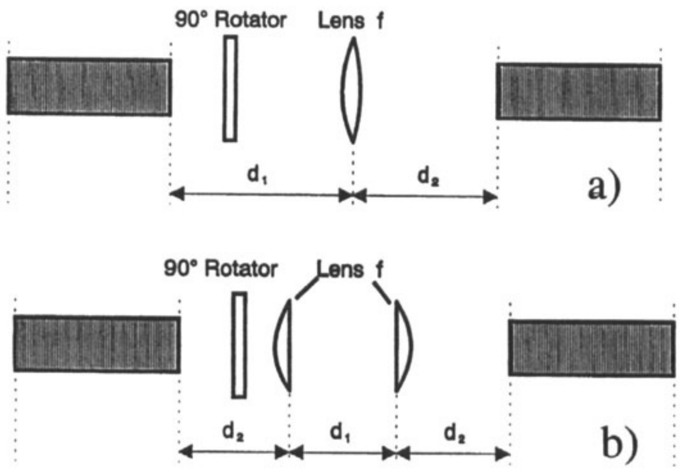

Fig. 8.22 Birefringence-compensated laser confi-gurations using a 90° polarization rotator and transformation optics. a) single lens scheme, b) dual lens scheme [3.199] (© Chapman & Hall 1996).

Note that (8.37), which holds only for $f \geq \ell/(2n_0)$, does not represent an imaging of the principal planes of the rods. This compensation technique is also applicable to the single rod resonator of Fig. 8.18b. If d denotes the distance of the HR mirror to the rod end face, the radius of curvature ρ of the mirror can be determined by setting $f=\rho/2$ in (8.37). The final result for the mirror curvature reads:

$$\rho = d + \frac{\ell}{2n_0} + \left[\frac{\ell}{2n_0}\right]^2 \frac{1}{d+\ell/(2n_0)} \tag{8.38}$$

A similar technique to compensate birefringence in a single rod resonator with two Faraday rotators is described in [3.209]. Here a lens-mirror combination is used to image the rod's principal plane onto itself.

b) Dual Lens Scheme (Fig. 8.22b)

Two of the three parameters d_1,d_2 and f can be chosen freely by using the condition:

$$[f-d_2-\frac{\ell}{2n_0}][d_1f+d_2f-d_1d_2] + \frac{\ell}{2n_0^2}[2n_0f^2-2\ell f+\ell d_1] = 0 \tag{8.39}$$

If we choose $d_1=2f$ (adjusted telescope), (8.39) will be met if:

$$d_2 = f - \ell/2n_0 \tag{8.40}$$

This means that the principal planes of the rods are imaged onto each other in this case.

Figure 8.23 presents measured depolarization losses for different dual Nd:YAG rod configurations as a function of the electrical pump power per rod. The 6x3/8 inch rods were placed between crossed polarizers and the transmitted power fraction of a collimated HeNe laser beam at λ=632.8nm was measured. This graph indicates the importance of using transformation optics in birefringence compensation schemes. With a polarization rotator alone the compensation works only at very low pump powers and the loss quickly rises to the maximum value of 27%. The remaining incomplete compensation for configuration C and D arises mainly as the result of rod end effects.

In recent years, birefringence compensation using one of the techniques described above has gained widespread application in solid state lasers, especially in dual rod Nd:YAG laser systems [3.200,3.201,3.206,3.208,3.210,3.213]. The main reason for this development is the need for high output power at near diffraction limited beam quality. Power scaling of TEM_{00} mode rod lasers beyond 50W can only be realized by increasing the number of rods. Since the TEM_{00} mode is only defined for linear polarization, compensation of the birefringence is mandatory. Average TEM_{00} mode output powers of up to 208W have been demonstrated with diode-pumped dual rod Nd:YAG lasers [3.206,3.210,3.213].

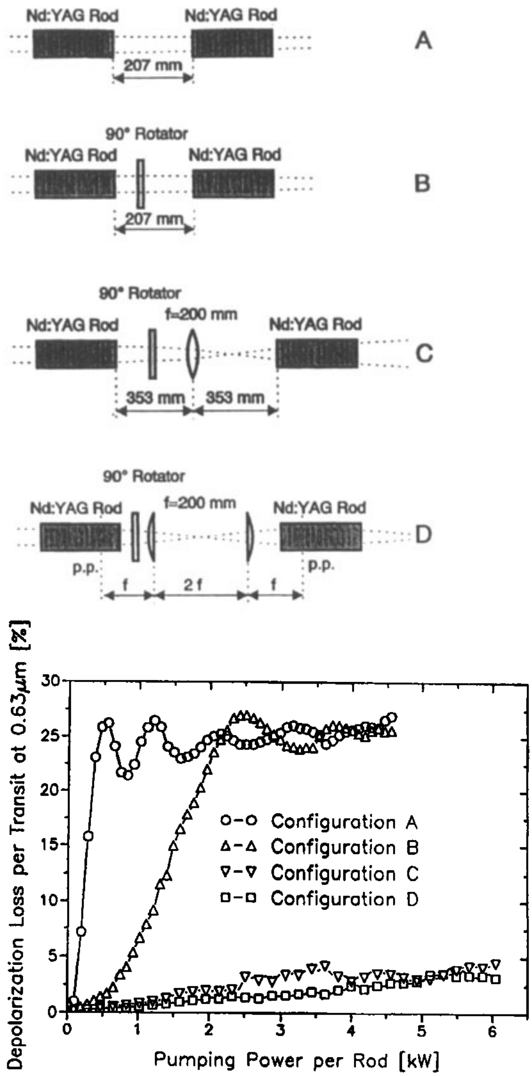

Fig. 8.23 Comparison of measured depolarization losses for four different birefringence compensation schemes of a dual Nd:YAG rod laser system as a function of the average pump power per rod. The 6x3/8 inch Nd:YAG rods were flashlamp pumped with a pump energy of 40J per rod and a pulse duration of 1ms. The pump power was varied with the repetition rate. The configurations were placed between crossed polarizers and the transmitted power fraction of a HeNe laser was measured [3.199] (© Chapman and Hall 1996).

Part IV

Open Resonators with Gain